Articles

Propagation of PAMAM Dendrons on Silica Gel: A Study on the Reaction Kinetics

Jie Bu,* Ruijiang Li, Chee Wee Quah, and Keith J. Carpenter

Institute of Chemical and Engineering Sciences (ICES), No. 1 Pesek Road, Jurong Island, Singapore 627833

Received March 10, 2004; Revised Manuscript Received May 19, 2004

ABSTRACT: Propagation of PAMAM (polyamidoamine) dendrons on solid spherical silica gel was achieved by a series of alternate Michael addition and amidation reactions. The reaction kinetics studies were investigated quantitatively. A newly developed method of immobilizing inert 3-(triethoxysilyl) propionitrile (TESPN) on silica before construction of PAMAM dendrons provided an internal standard to normalize drift IR spectra for kinetics studies. A reaction kinetic model was proposed on the basis of IR spectra and TGA measurements. The simulated results match with the experimental data and confirm consistency with the proposed kinetic model that a "cross-linking" reaction occurred in amidation generating structural defects, and steric hindrance existed during the Michael addition reaction. Furthermore, we found that the TESPN immobilized on silica acted as a "spacer" to reduce the initial density of amino groups on silica and improved the synthesis efficiency remarkably. The reaction kinetics study in this paper is instrumental to the optimization of the synthesis of PAMAM dendrons on solid surface.

Introduction

Dendrimers are cascade-branched, highly defined macromolecules, characterized by a combination of high end-group functionality and compact molecular structures. Since the seminal works in this field, a large number of dendrimer structures have been developed, and scientists from different interdisciplinary fields have made intense efforts into the studies of dendrimers.[1−11]

Polyamidoamine dendrimers (PAMAM) represent an exciting new class of macromolecular architecture called "dense star" polymers which have a high degree of molecular uniformity, narrow molecular weight distribution, specific size and shape characteristics, and highly functionalized terminal amino groups. The structural precision of PAMAM dendrimers has motivated numerous studies aimed at biomedical applications, for example, drug carriers[12] and DNA delivery.[13] However, because the synthesis of dendrimers involves a series of repetitive steps starting with a central initiator core, the synthetic construction of dendrimers becomes a significantly tedious and time-consuming work. Moreover, excess reagents that are required to drive reactions to completion in homogeneous reaction may render subsequent purification difficult. In contrast, the solid-phase synthesis of PAMAM dendrons becomes a remarkably powerful tool as these excess reagents can be removed easily by simple washing.

Swali et al.[14] described the solid-phase synthesis of PAMAM dendrons starting from a resin bead. An acid-labile linker attached to a polyamine scaffold was used to allow cleavage of the dendrons from the resin to monitor the synthesis.[15] Shortly after that, grafting of PAMAM dendrons on silica gel was also reported,[16] and subsequently silica-supported PAMAM dendrons have been widely investigated to explore its applications in catalysis[17−19] and chiral separations.[20] However, incomplete reactions and structural defects were investigated as the construction of PAMAM dendrimer by stepwise synthesis in liquids.[10,11,21−28] On the other hand, several researchers have reported these structural defects during propagation of PAMAM dendrons on solid phse.[29,30] So far, there are not many investigations reported on the monitoring of the reactions at the solid−liquid interface, reaction kinetics study, and controlling the level of structural defects for the synthesis of dendritic polymer. Infrared (IR) spectroscopy is a powerful tool to investigate the organic reaction because IR is sensitive to some specific functional groups on solid surface during reaction. The purpose of this study is to monitor all synthesis steps by IR spectroscopy to investigate the completion of reactions. On the basis of the experimental data, we propose a reaction kinetics model and discuss the presence of possible structural defects in PAMAM dendrons.

Experimental Section

Materials and Reagents. To synthesize solid-phase PAMAM dendrons, ultrapure spherical silica gel (SiliCycle) was used as the starting material. Its particle size, specific surface area, and pore size are 15 μm, 270 m^2/g, and 100 Å, respectively. Silica gel was first dried in a tube oven at 110 °C before use. 3-(Triethoxysilyl)propionitrile (TESPN) and 3-aminopropyltriethoxylsilane (APES) were used without further purification. Methyl acrylate (MA) (Aldrich) was dried over sodium sulfate and distilled before use. Ethylendiamine (EDA) (J. T. Baker) was refluxed over sodium and distilled before use.

* To whom correspondence should be addressed. E-mail: bu_jie@ices.a-star.edu.sg.

10.1021/ma040055b CCC: $27.50
Published on Web 08/14/2004

Scheme 1. Preparation of an "Initiator Site" G0: (a) Nitrile Grafted on Silica Gel, and (b) Initiator G0

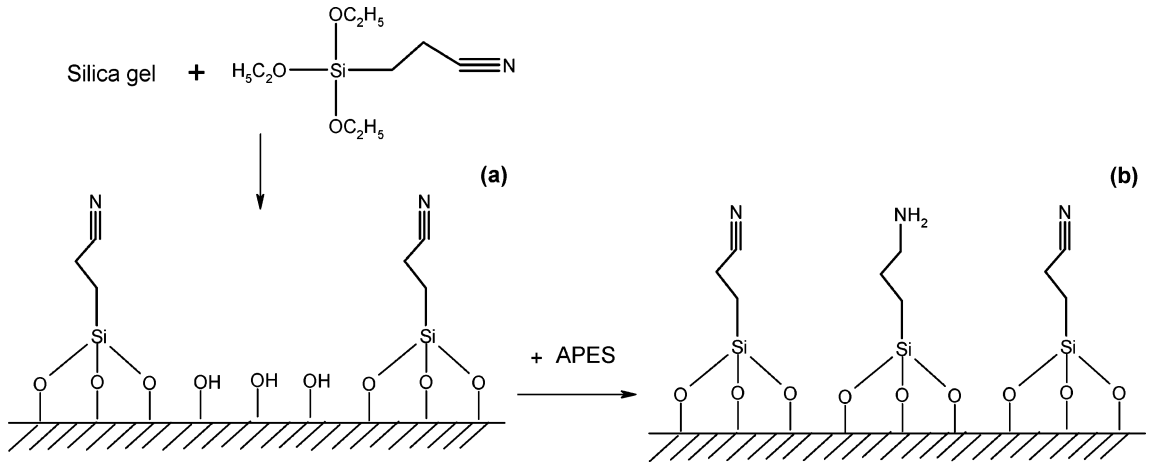

Scheme 2. Synthesis of PAMAM Dendrons: (A) Michael Addition of MA to the Amine Termini To Produce G0.5, G1.5, and G2.5, and (B) Amidation of the Ester Moieties by EDA To Generate G1, G2, and G3 Dendrons, Respectively

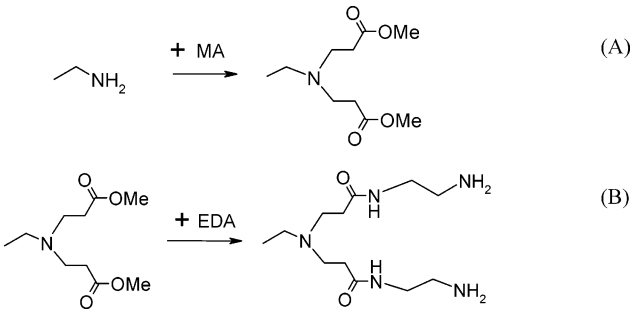

Scheme 3. Theoretical Structure of PAMAM−SiO_2 Dendrons for Third Generation (G3)

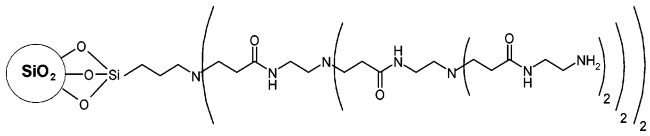

Propagation of PAMAM Dendrons from Silica Surface. The dendron propagation method pioneered by Tsubokawa and co-workers [16] was modified to construct the dendrons. Before the introduction of amino groups, the internal standard material, TESPN, was first immobilized onto the silica gel. In a 250 mL flask were mixed 10 g of silica gel, 25 mL of TESPN, and 150 mL of toluene, which was stirred at 110 °C and refluxed for 6 days. After the reaction, the mixture was centrifuged and the excess reagents in the precipitate were extracted with toluene for 24 h using Soxhlet apparatus. The resultant silica labeled with the nitrile (−CN) group was dried in vacuo at 120 °C to remove liquid phases. The preparation of an "initiator site" (G0) through introduction of amino groups onto the silica surface was achieved by reacting the remaining surface silanol groups with APES. This reaction was carried out at 110 °C in toluene for 48 h. The immobilization of TESPN and APES is illustrated in Scheme 1.

PAMAM dendrons were then constructed by the repetitive additions of a branching unit onto this G0 core. Michael addition of MA to the terminal amine on G0 generated amino propionate esters (G0.5). Subsequent amidation of the ester moieties with EDA eventually completed the first generation (G1). All branching occurred at the terminal amine as shown in Scheme 2.

Finally, repetitive Michael addition and amidation reactions yielded third generation (G3) PAMAM dendrons. During the syntheses, excess reagents (MA and EDA) were fed into batch reactor to drive reactions to completion. Michael addition reactions were carried out at 60 °C in toluene, and amidation reactions were carried out at 60 °C in methanol. Vacuum filtration, extraction by Soxhlet apparatus, and drying in vacuo are carried out to remove excess reagents. The theoretical structure of G3 PAMAM−SiO_2 dendrons is shown in Scheme 3.

Surface Analysis. During each synthesis step, a series of solid samples were collected at regular time intervals. To remove excess liquid phase, the solid sample was filtered in syringe filters several times and then dried in vacuo at 120 °C for 2 h, after which it was analyzed using diffuse reflectance infrared Fourier transform (drift) spectroscopy (Bruker, Equinox 55). The measurements were carried out for 100 scans and at 4 cm^{-1} resolution. Continuous nitrogen purging of IR instrument was maintained before and during the sample scanning.

The amount of dendrons grafted onto silica surface was measured by a thermogravimetric analyzer (Perkin-Elmer TGA-7). Specifically, before TGA measurement, each sample was dried in vacuo at 120 °C for 2 h to remove excess organic liquid phase, and then the sample (15 mg) was loaded into TGA aluminum crucible. Using 200 mL/min airflow, the sample was first heated to 110 °C, held for 10 min to remove surface water, and then subjected to a constant temperature ramp of 5 °C/min to 700 °C, which has been demonstrated to be sufficiently high to remove all surface-bonded organosilanes.[31] The weight loss profiles were then observed to reach a plateau quickly at the beginning of the 110 °C drying period, indicating removal of surface water before the start of the heating ramp. The amount of grafted organic phase was calculated by the weight difference between 110 and 700 °C.

Surface morphology changes, as a result of dendron propagation, were observed using a field emission scanning electron microscope (FE-SEM, JEOL, JSM-6700F). Emission current was set at 10 μA, working distance was set at 8 mm, and accelerating voltage was set at 2 kV. Sample preparation involves coating the specimen crucible with conductive carbon paint and sprinkling solid PAMAM−SiO_2 G3 dendrons onto the surface for SEM imaging.

Results and Discussion

Surface Analysis and Drift IR Spectra. Figure 1 shows the SEM photos of the silica gel before and after grafting of dendrons onto silica. The photo in Figure 1b clearly indicates the changes in the surface of silica gel after successful construction of G3 dendrons on the silica.

As described earlier, the dendron synthesis process is a series of repetitive reaction steps starting with a central initiator core. In this study, the bare silica gel was labeled with nitrile and amino groups first, and then it was used as starting material (G0) to construct

(a)

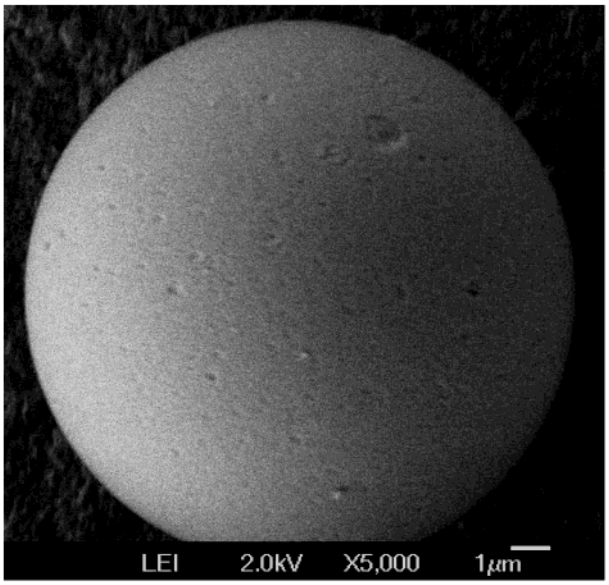

(b)

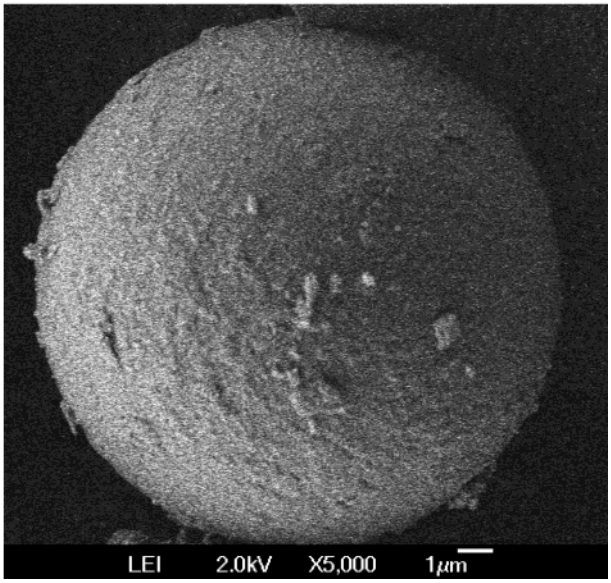

Figure 1. Silica-supported PAMAM dendrons: (a) bare spherical silica gel, and (b) after PAMAM dendrons were grafted onto silica gel.

dendrons. Figure 2 presents the drift IR spectra of solid samples collected at different reaction time intervals. It is worth noting that there was a distinguished band at 2260 cm^{-1} after immobilizing TESPN on silica. This band is assigned to the nitrile (−CN) stretching vibration, and there is no leaching of nitrile group observed in the subsequent Michael addition and amidation reactions. This strongly suggests that TESPN was successfully and firmly grafted onto the silica. Thus, the nitrile IR band could be taken as the internal standard band.

To compare the intensity of all bands observed, all IR spectra were normalized with the intensity of the nitrile band at 2260 cm^{-1}. Before the Michael addition reaction started ($t = 0$), one IR band at ca. 1640 cm^{-1}, which is characteristic of amine ($-NH_2$), can be clearly observed, indicating the amine on the surface of G0.

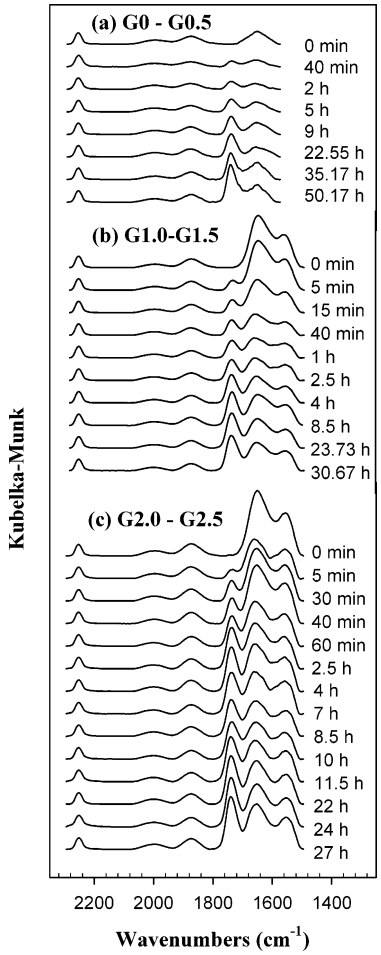

Figure 2. Drift IR spectra of Michael addition.

During the reaction, a new band at ca. 1730 cm^{-1}, assignable to the ester (−COOMe),[32] appeared and increased with reaction time. Similarly, the increase in the intensity of ester band could be observed in Figure 2b and c, which shows the IR spectra of the samples reacting with MA to form G1.5 and G2.5 dendrons, but the increasing rate of IR intensity seems to be higher.

In Figure 3a, amidation of G0.5 ester moieties with EDA generates G1 dendrons, resulting in increasing amide band and correspondingly decreasing ester band intensities. In contrast to Figure 2, two new appearing IR bands at 1655 and 1550 cm^{-1} assignable to amide I and amide II groups[32] were observed. G2 and G3 dendrons were similarly constructed by reacting G1.5 and G2.5 samples with EDA, respectively. From Figure 3b and c, it was found that the ester band gradually disappeared, while the amide bands became stronger. It is worth noting that the ester peak decreased from the start and totally vanished at the end, which indicates that the amidation step is complete under current conditions.

In summary, the changes in the intensity of the ester band (Figures 2 and 3) clearly reflect the alternate Michael addition and amidation reactions during construction of PAMAM dendrons on silica gel. However, to investigate the extent of these reactions, quantitative analysis is required.

Grafted Amount. The grafted amounts of dendrons on silica for each generation were obtained by TGA measurements and are listed in Table 1. During each

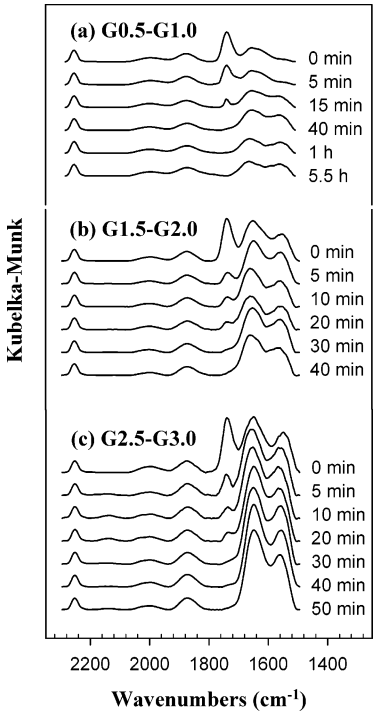

Figure 3. Drift IR spectra of amidation.

Table 1. Grafted Amount As Determined by TGA

synthesis stage	weight loss %[a]	grafted amount (mg/g SiO_2)	theoretical value (mg/g SiO_2)
nitrile grafted silica	10.664		
G0	11.96	12.9	12.9
G0.5	15.19	45.2	51.3
G1	16.38	57.2	63.8
G1.5	22.49	118.2	140.5
G2	23.36	126.9	165.5
G2.5	30.89	202.2	318.9
G3	32.10	214.3	368.8

[a] Determined by the TGA weight-loss profile and calculated on the basis of 1 g of silica; weight loss % = (weight at 110 °C − weight at 700 °C)/weight at 700 °C × 100%.

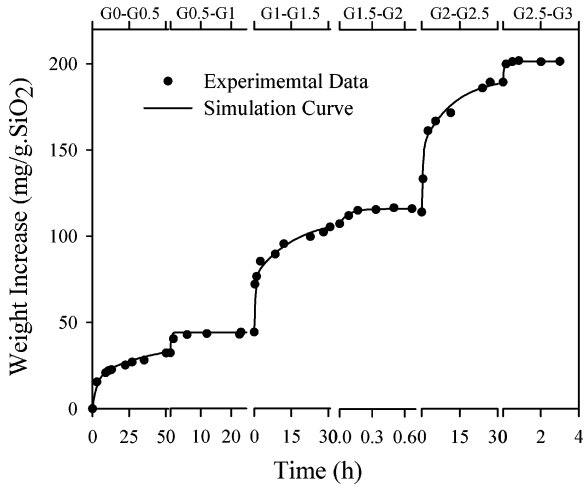

Figure 4. TGA profile of PAMAM dendrons.

individual generation stage, all weight changes are clearly illustrated in Figure 4.

The weight increase of organic phase was calculated on the basis of 1 g of SiO_2. From Table 1, despite that the grafted amounts for each generation step increased with time, it is smaller than the theoretical value. First, we can see this, especially in Figure 4 whereby the increase in grafted amount for each amidation step is surprisingly small even though the drift spectra (Figure 3) clearly illustrated complete amidation reaction. Second, in theoretical terms, during amidation, one terminal amine group ($-NH_2$) of EDA only reacts with one ester group, resulting in regeneration of amine termini (Scheme 2) and an increase in the grafted amount. However, these increases of grafted amounts in G1, G2, and G3 are much smaller than the expected values. This implies that possible side reactions were occurring during these synthesis steps. Therefore, it is necessary to investigate the reaction kinetics.

Proposed Reaction Kinetics Model. Several research groups have described and characterized the side reactions and possible structural "errors" in PAMAM dendrimers.[10,11,21−28] ESI FT-ICR MS analysis,[22] MALDI-TOF MS analysis,[11,26] and capillary zone electrophoresis (CZE) separation[24] of dendrimers indicated that side reactions gave rise to three types of structural "errors" − missing arm, dimer, and intramolecular cyclization. According to these studies, we proposed a "cross-linking" reaction model for the amidation step during grafting of PAMAM dendrons on silica gel. As illustrated in Scheme 4, two adjacent ester groups could be linked by reacting with one EDA molecule, resulting in structural defects, comparable to dimer and intramolecular cyclization described in previous articles.[11,22,24]

The amidation process, consisting of two series-parallel reactions, is illustrated in Scheme 5.

According to Scheme 5, two ester groups (bonding on solid phase) react with one EDA molecule and generate two methanol molecules, which are removed after drying. The amide group on dendrons (R) is the desired product. Reaction a causes a 28 g weight increase based on 1 mol of reactant. However, reaction b results in extra weight decrease in grafted amount, due to removal of methanol (32 g/mol). In other words, the more S generated, the smaller the actual weight increase. As a result, this side reaction causes structural defects and the grafted amount to be less than the theoretical value, even though the reaction between ester and amine groups was complete (Figure 3).

Because excessive EDA was fed in, the general representation of these reactions is

$$\mathrm{E} \xrightarrow[+\mathrm{EDA}]{k_{\mathrm{A1}}} \mathrm{R} \qquad \text{(R1)}$$

$$\mathrm{R} + \mathrm{E} \xrightarrow{k_{\mathrm{A2}}} \mathrm{S} \qquad \text{(R2)}$$

and the rate expressions are given by

$$\frac{\mathrm{d}C_{\mathrm{E}}}{\mathrm{d}t} = -C_{\mathrm{E}}(k_{\mathrm{A1}} + k_{\mathrm{A2}}C_{\mathrm{R}}) \qquad (1)$$

$$\frac{\mathrm{d}C_{\mathrm{R}}}{\mathrm{d}t} = C_{\mathrm{E}}(k_{\mathrm{A1}} - k_{\mathrm{A2}}C_{\mathrm{R}}) \qquad (2)$$

$$\frac{\mathrm{d}C_{\mathrm{S}}}{\mathrm{d}t} = k_{\mathrm{A2}}C_{\mathrm{R}}C_{\mathrm{E}} \qquad (3)$$

where the C_{i} is the molar concentration of each functional group and k_{i} represents reaction rate constant.

On the other hand, incomplete Michael addition[11,24] may lead to missing arm structures during grafting of PAMAM dendrons on silica gel; the reaction steps can be illustrated in Scheme 6.

Scheme 4. Structural Defects Caused by the Cross-Linking Reaction

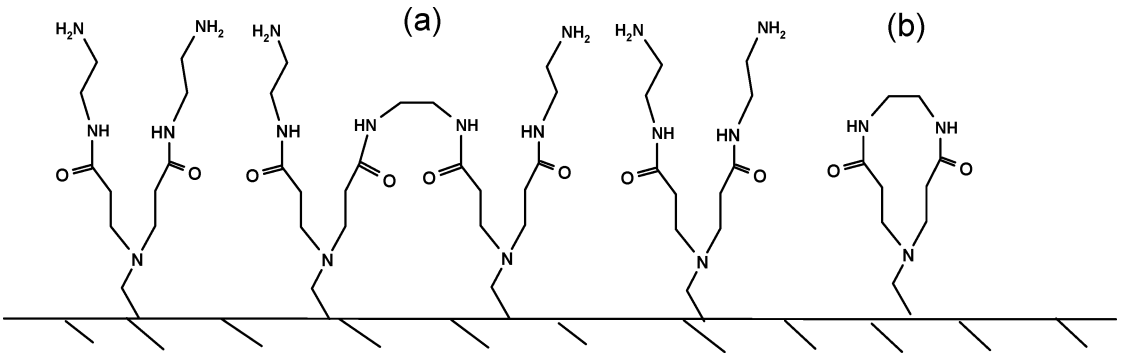

Scheme 5. Amidation Reaction

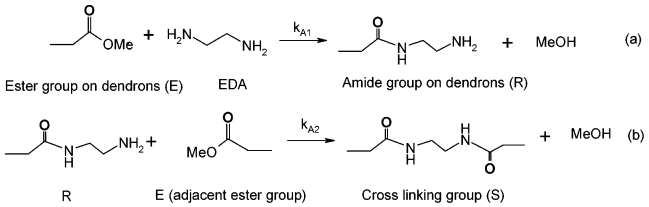

Scheme 6. Michael Addition of Methyl Acrylate to Amine

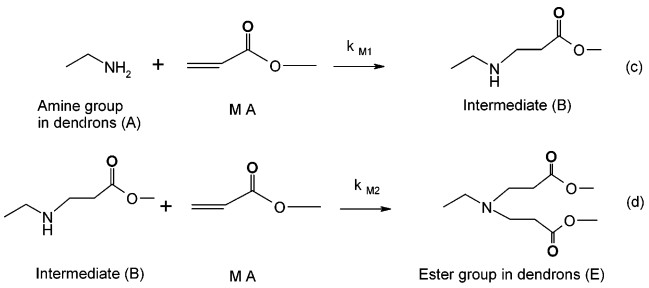

Because excessive MA was fed in, the above reactions become series pseudo-first-order reactions, and the general representation of these reactions is

$$\mathrm{A} \xrightarrow[+\mathrm{MA}]{k_{\mathrm{M1}}} \mathrm{B} \xrightarrow[+\mathrm{MA}]{k_{\mathrm{M2}}} \mathrm{E} \qquad \text{(R3)}$$

and the ester group on the dendrons (E) is the desired product. The rate expressions are given by

$$\frac{\mathrm{d}C_{\mathrm{A}}}{\mathrm{d}t} = -k_{\mathrm{M1}}C_{\mathrm{A}} \qquad (4)$$

$$\frac{\mathrm{d}C_{\mathrm{B}}}{\mathrm{d}t} = k_{\mathrm{M1}}C_{\mathrm{A}} - k_{\mathrm{M2}}C_{\mathrm{B}} \qquad (5)$$

$$\frac{\mathrm{d}C_{\mathrm{E}}}{\mathrm{d}t} = k_{\mathrm{M2}}C_{\mathrm{B}} \qquad (6)$$

Simulation of Experimental Results. According to the reaction model for the Michael addition shown in Scheme 6, there is one methyl ester group existing in intermediate B and there are two in the final product E. Thus, the concentration of methyl ester is directly proportional to the summation of C_{B} and $2C_{\mathrm{E}}$, while the intensity of the band at 1730 cm^{-1} detected by drift spectroscopy is proportional to the concentration of methyl ester. They could be expressed by

$$I_{--\mathrm{COOMe}} \propto C_{-\mathrm{COOMe}} \propto C_{\mathrm{B}} + 2C_{\mathrm{E}} \qquad (7)$$

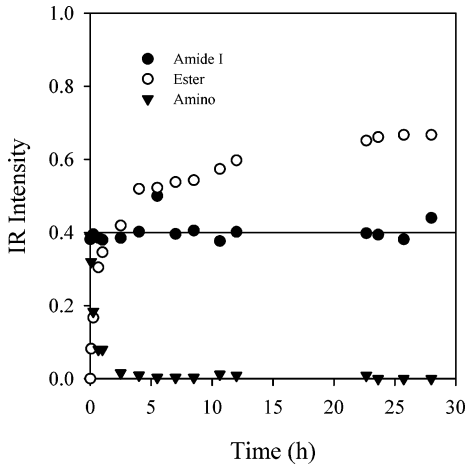

Figure 5. Reaction profile (G1−G1.5) obtained from drift IR spectra.

where the $I_{--\mathrm{COOMe}}$ represents the intensity of the IR band for the methyl ester group. On the other hand, because the intermediate B and product E groups contributed to the weight increase, the increase in grafted amount for the Michael addition step could be expressed by

$$\Delta W_{\mathrm{addition}} \propto C_{\mathrm{B}} + 2C_{\mathrm{E}} \qquad (8)$$

where the $\Delta W_{\mathrm{addition}}$ is the weight increase in grafted amount and can be measured by TGA. Therefore

$$I_{--\mathrm{COOMe}} \propto \Delta W_{\mathrm{Addition}} \qquad (9)$$

The differential equations (eqs 4−6) and eq 9 could be solved by the numerical method. According to the TGA measurements (Table 1), the initial concentration of Ao (amino group) before construction of G0.5 was calculated as 0.223 mmol/g of SiO_2. By simulation of the TGA experimental data, the reaction rate constants, k_{M1} and k_{M2}, for the first synthesis step (G0−GG0.5) were obtained. The simulation curves (solid lines) matched the TGA data (black dot points) very well as shown in Figure 4. Subsequently, we should compare the simulation results with the drift IR data.

The original measured drift IR spectra (Figures 2 and 3) were treated and analyzed by using OPUS software supplied by Bruker. The intensities of the ester, amino, and amide bands were calculated and separated by the curve-fitting method. Figure 5 displays the peak fitting results for analysis of the dendrons construction step from G1 to G1.5. The TGA, IR experimental data, and simulation results were combined and plotted in Figure

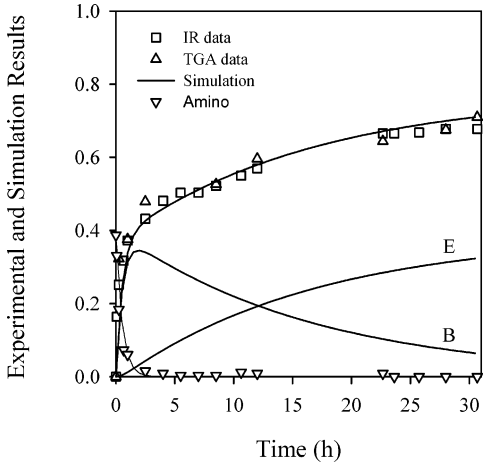

Figure 6. Reaction profile (G1−G1.5) obtained from drift IR spectra, TGA data, and simulation.

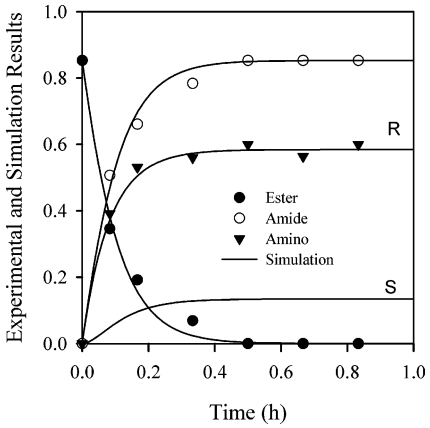

Figure 7. Reaction profile (G2.5−G3) obtained from drift IR spectra and simulation.

6. It was found that the IR data (□) showed proportionality to the TGA data (△) as predicted in eq 9 and the simulation curves matched these experimental data very well.

For amidation reactions (Scheme 5), because the side reaction generates the cross-linking group S, the net weight increase in grafted amount could be expressed as

$$\Delta W_{\text{amidation}} = 28C_{\text{R}} - 32C_{\text{S}} \qquad (10)$$

By simulation of the TGA experimental data, followed by solving the differential equations (eqs 1−3) and eq 10 numerically, we can obtain reaction rate constants, k_{A1} and k_{A2}. Figure 7 presents the experimental and simulation values for the dendron construction step from G2.5 to G3. All simulation work should be done following the order

$$\text{G0}-\text{G0.5} \rightarrow \text{G0.5}-\text{G1} \rightarrow \text{G1}-\text{G1.5} \rightarrow \text{G1.5}-\text{G2} \rightarrow \text{G2}-\text{G2.5} \rightarrow \text{G2.5}-\text{G3}$$

The simulation results are summarized in Table 2. Furthermore, the experimental data (dot point) and simulation curves (solid line) for all construction steps, from G0 to G3, were plotted in Figure 8. This plot clearly illustrates the conversion profiles of ester and amino groups in Michael addition and amidation reactions. It is worth noting that, for each synthesis step, the simulation curve matches the TGA and drift IR experimental data. This strongly suggests that the proposed reaction kinetics model is reasonable.

Table 2. Simulation Results of the Reaction Rate Constant

synthesis procedure	reaction step	reaction rate constant k_{M1} (h^{-1})	reaction rate constant k_{M2} (h^{-1})	functional groups (mmol/g SiO_2) amino	functional groups (mmol/g SiO_2) ester group
Michael addition	G0−G0.5	0.35	0.026	0.2230[a]	0.0
	G1−G1.5	1.85	0.060	0.3870	0.0
	G2−G2.5	2.20	0.065	0.4536	0.0
		k_{A1} (h^{-1})	k_{A2}[b]	ester group	amino
amidation	G0.5−G1	3.00	0.05	0.3900	0.3870
	G1.5−G2	5.52	4.87	0.7098	0.4536
	G2.5−G3	8.51	5.07	0.8529	0.6000

[a] Determined by TGA measurement. [b] The unit of k_{A2} corresponds to the second-order reaction.

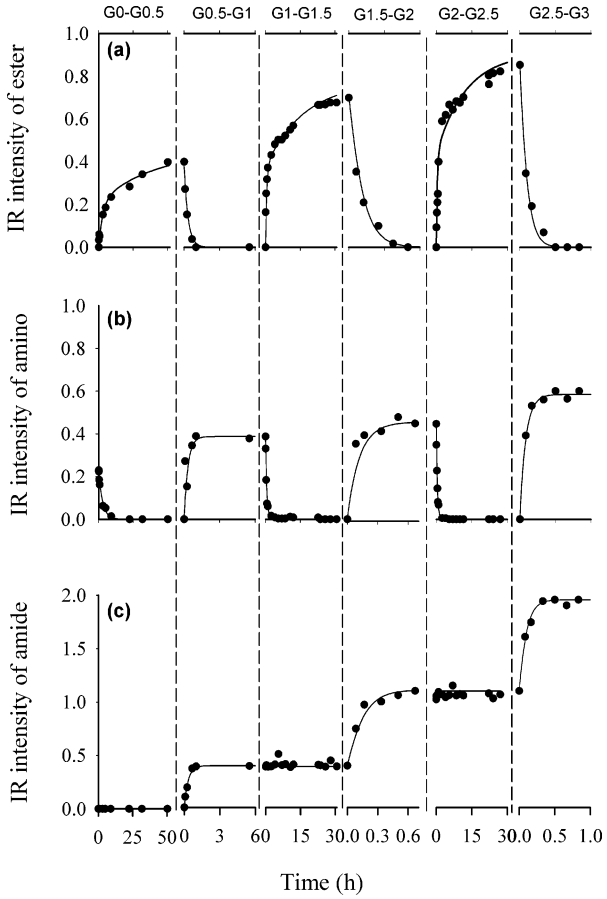

Figure 8. Reaction conversion profile obtained from drift IR spectra of the synthesis of PAMAM dendrons.

The overall reaction rates of Michael addition and amidation at higher generation are larger than those at lower generation (Figure 8a,b). This is because the local concentration reactant doubles (roughly) in every generation, which should increase the overall reaction rate.

We also noted that the concentration of the amide group (−CONH) remains constant during the Michael addition step (Figure 8b), which is consistent with the proposed reaction model, as the amide group generated from the previous amidation step does not involve the Michael addition reaction.

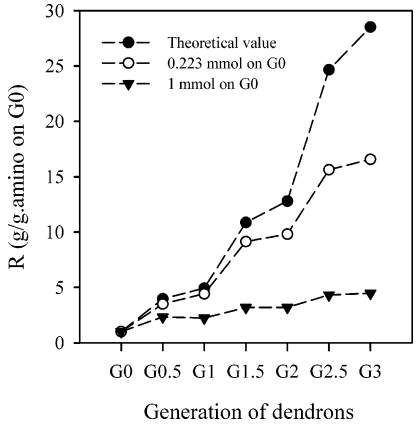

Figure 9. Influence of initial amino concentration.

Structural Defects. From Table 2, the "cross-linking" reaction is obvious and is in agreement with previous studies,[11,22,24] although the k_{A2} value of reaction b is smaller than the k_{A1} value of the desired reaction a (Scheme 5). The undesired cross-linking reaction b reduces the amount of amine groups in amine termini. As a result, it has a significant cumulative effect on subsequent synthesis steps because the subsequent Michael addition reaction branching occurs only at the available terminal amine on higher generation dendrons (G1 and G2).

We particularly note that, for the series reactions in the Michael addition (Scheme 6), the steric hindrance created by the ester group in the secondary amine moiety hinders the approach of the MA molecule to the nucleophilic nitrogen center, thereby slowing down the reaction rate. Therefore, the k_{M2} value of reaction d is much smaller than k_{M1} (Table 2), resulting in some remaining intermediate B (Figure 6). Peterson et al.[11] suggested that this missing arm structure may arise from both the incomplete Michael reaction and the retro-Michael reaction.

Effect of Initial Amino Group Content on the Construction of Dendrons. Figure 9 shows the effect of initial amino group content on the construction of dendrons from silica surface; *R* is the ratio of the grafted amount to the initial amino group content (Ao). It was found that the *R* value for the silica having 0.223 mmol of amino groups was much higher than that of 1 mmol of amino group at higher generations of dendrons. This indicates that the efficiency of the synthesis of dendrons from silica surface, starting with a low density of amino groups, has been significantly improved although the *R* value is still lower than the theoretical value.

This is in agreement with the proposed cross-linking reaction model; a low initial concentration of amino group decreases crowding and subsequently reduces the formation of cross-linking structures (defect "a" in Scheme 4) at higher generations of dendrons. Peterson et al.[11] pointed out that this type of dimeric structure appeared in higher generations of dendrimer. With this point of view, the TESPN immobilized on silica not only provides an internal IR standard band to normalize drift IR spectra but also acts as a "spacer" to reduce the initial density of amino groups (Scheme 1), thereby improving the synthesis efficiency.

Conclusions

Prior to the construction of dendrons on silica gel, TESPN was immobilized onto the surface of silica gel with the appearance of distinctive nitrile (−CN) IR band at 2260 cm^{-1}. Subsequently, the G3 solid PAMAM dendrons were propagated by the repetitive additions of a branching unit onto the nitrile labeled silica gel. All synthesis steps were monitored by drift IR spectroscopy. Because no leaching of the nitrile group was observed, the nitrile IR band was taken as an internal standard to normalize all IR spectra and investigate the reaction kinetics. TGA measurements were also used as a reference to determine the amount of grafted dendrons quantitatively.

The IR spectra and TGA experimental data showed that the ester group and the grafted dendron amounts were changing as a function of reaction time. A reaction kinetics model for Michael addition and amidation was proposed and matched with the experimental data. The experimental results suggest that the "cross-linking" reaction occurring in amidation processes generated structural defects, which has a significant cumulative effect on the subsequent synthesis steps, causing significant reduction in the construction of dendrons. In addition, the analysis of reaction rate constants indicates that Michael addition of MA to diamine is hindered by steric crowding, resulting in incomplete propagation of dendrons on silica gel. Furthermore, it was found that propagation of dendrons on silica surface with a low density of amino groups (achieved by −CN group immobilization) is more effective than one with a high density of amino groups.

Our research work on the kinetics study of the solid−liquid surface reaction aided by drift IR spectroscopy and TGA analysis is instrumental to the optimization of the construction of PAMAM dendrons. This paper is the first report on the use of the internal standard IR band to normalize IR spectra.

References and Notes

(1) Vogtle, F.; Gestermann, S.; Hesse, R.; Schwierz, H.; Windisch, B. *Prog. Polym. Sci.* **2000**, *25*, 987−1041.
(2) Hecht, S.; Frechet, J. M. J. *Angew. Chem., Int. Ed.* **2001**, *40*, 74−91.
(3) Oosterom, G. E.; Reek, J. N. H.; Kamer, P. C. J.; Van Leeuwen, P. *Angew. Chem., Int. Ed.* **2001**, *40*, 1828−1849.
(4) Choi, H. C.; Kim, W.; Wang, D. W.; Dai, H. J. *J. Phys. Chem. B.* **2002**, *106*, 12361−12365.
(5) Stiriba, S. E.; Frey, H.; Haag, R. *Angew. Chem., Int. Ed.* **2002**, *41*, 1329−1334.
(6) Van Heerbeek, R.; Kamer, P. C. J.; Van Leeuwen, P.; Reek, J. N. H. *Chem. Rev.* **2002**, *102*, 3717−3757.
(7) Zimmerman, S. C.; Wendland, M. S.; Rakow, N. A.; Zharov, I.; Suslick, K. S. *Nature* **2002**, *418*, 399−403.
(8) Bertorelle, F.; Lavabre, D.; Fery-Forgues, S. *J. Am. Chem. Soc.* **2003**, *125*, 6244−6253.
(9) Tomalia, D. A. *Nat. Mater.* **2003**, *2*, 711−712.
(10) Tomalia, D. A.; Naylor, A. M.; Goddard, W. A., III. *Angew. Chem., Int. Ed. Engl.* **1990**, *29*, 138−175.
(11) Peterson, J.; Allikmaa, V.; Subbi, J.; Pehk, T.; Lopp, M. *Eur. Polym. J.* **2003**, *39*, 33−42.
(12) Beezer, A. E.; King, A. S. H.; Martin, I. K.; Mitchel, J. C.; Twyman, L. J.; Wain, C. F. *Tetrahedron.* **2003**, *59*, 3873−3880.
(13) Luo, D.; Haverstick, K.; Belcheva, N.; Han, E.; Saltzman, W. M. *Macromolecules* **2002**, *35*, 3456−3462.
(14) Swali, V.; Wells, N. J.; Langley, G. J.; Bradley, M. *J. Org. Chem.* **1997**, *62*, 4902−4903.
(15) Marsh, I. R.; Smith, H.; Bradley, M. *Chem. Commun.* **1996**, *8*, 941−942.
(16) Tsubokawa, N.; Ichioka, H.; Satoh, T.; Hayashi, S.; Fujiki, K. *React. Funct. Polym.* **1998**, *37*, 75−82.
(17) Bourque, S. C.; Maltais, F.; Xiao, W. J.; Tardif, O.; Alper, H.; Arya, P.; Manzer, L. E. *J. Am. Chem. Soc.* **1999**, *121*, 3035−3038.
(18) Bu, J.; Judeh, Z. M. A.; Ching, C. B.; Kawi, S. *Catal. Lett.* **2003**, *85*, 183−187.

(19) Chung, Y. M.; Rhee, H. K. *Catal. Lett.* **2003**, *85*, 159−164.
(20) Driffield, M.; Goodall, D. M.; Klute, A. S.; Smith, D. K.; Wilson, K. *Langmuir* **2002**, *18*, 8660−8665.
(21) Tomalia, D. A.; Baker, H.; Dewald, J. R.; Hall, M.; Kallos, G.; Martin, S.; Roeck, J.; Ryder, J.; Smith, P. *Polym. J.* **1985**, *17*, 117−132.
(22) Tolic, L. P.; Anderson, G. A.; Smith, R. D.; Brothers, H. M.; Spindler, R.; Tomalia, D. A. *Int. J. Mass Spectrom. Ion Processes* **1997**, *165*, 405−418.
(23) Brothers, H. M.; Piehler, L. T.; Tomalia, D. A. *J. Chromatogr., A* **1998**, *814*, 233−246.
(24) Ebber, A.; Vaher, M.; Peterson, J.; Lopp, M. *J. Chromatogr., A* **2002**, *949*, 351−358.
(25) Mansfield, M. L. *Macromolecules* **1993**, *26*, 3811−3814.
(26) Zhou, L.; Russell, D. H.; Zhao, M. Q.; Crooks, R. M. *Macromolecules* **2001**, *34*, 3567−3573.
(27) Smith, P. B.; Martin, S. J.; Hall, M. J.; Tomalia, D. A. In *Applied Polymer Analysis and Characterization*; Mitchell, J., Jr., Ed.; Hanser: München, 1987; pp 357−385.
(28) Kallos, G. J.; Tomalia, D. A.; Hedstrand, D. M.; Lewis, S.; Zhou, J. *Rapid Commun. Mass Spectrom.* **1991**, *5*, 383−386.
(29) Bourque, S. C.; Alper, H.; Manzer, L. E.; Arya, P. *J. Am. Chem. Soc.* **2000**, *122*, 956−957.
(30) Chung, Y. M.; Rhee, H. K. *Catal. Lett.* **2002**, *82*, 249−253.
(31) Chaimberg, M.; Parnas, R.; Cohen, Y. *J. Appl. Polym.Sci.* **1989**, *37*, 2921−2931.
(32) Wells, M.; Crooks, R. M. *J. Am. Chem. Soc.* **1996**, *118*, 3988−3989.

MA040055B